© 2018. Published by The Company of Biologists Ltd | Development (2018) 145, dev155317. doi:10.1242/dev.155317

RESEARCH REPORT

Microbiota promote secretory cell determination in the intestinal epithelium by modulating host Notch signaling

Joshua V. Troll*,[1], M. Kristina Hamilton[2], Melissa L. Abel‡,[1], Julia Ganz§,[2], Jennifer M. Bates¶,[1], W. Zac Stephens,[1], Ellie Melancon[2], Michiel van der Vaart[3], Annemarie H. Meijer[3], Martin Distel[4], Judith S. Eisen[2,‡‡] and Karen Guillemin[1,5,‡‡]**

ABSTRACT

Resident microbes promote many aspects of host development, although the mechanisms by which microbiota influence host tissues remain unclear. We showed previously that the microbiota is required for allocation of appropriate numbers of secretory cells in the zebrafish intestinal epithelium. Because Notch signaling is crucial for secretory fate determination, we conducted epistasis experiments to establish whether the microbiota modulates host Notch signaling. We also investigated whether innate immune signaling transduces microbiota cues via the Myd88 adaptor protein. We provide the first evidence that microbiota-induced, Myd88-dependent signaling inhibits host Notch signaling in the intestinal epithelium, thereby promoting secretory cell fate determination. These results connect microbiota activity via innate immune signaling to the Notch pathway, which also plays crucial roles in intestinal homeostasis throughout life and when impaired can result in chronic inflammation and cancer.

KEY WORDS: Microbiota, Notch, Myd88, Intestinal cell determination, Secretory cell, Zebrafish

INTRODUCTION

Host-associated microbiota play important roles in animal health and development (McFall-Ngai et al., 2013), yet the mechanisms by which they influence processes such as cell differentiation remain unknown. Understanding the relationship between microbiota and intrinsic developmental pathways is key for developing strategies to promote intestinal homeostasis in pathological situations. We showed previously that the microbiota is necessary to promote secretory fates in the larval zebrafish intestinal epithelium (Bates et al., 2006). Zebrafish larvae reared germ free (GF) have fewer secretory cells than their conventionally reared (CV) counterparts; this deficit is reversed by conventionalization (CVZ) of GF animals with zebrafish-associated microbes.

Intestinal secretory fate determination is regulated by Notch signaling across many species (Fre et al., 2011), including zebrafish (Crosnier et al., 2005) and mammals (Noah and Shroyer, 2013; Yuan et al., 2015). Intestinal stem cells differentiate into two primary cell types: absorptive enterocytes and secretory cells. Secretory cells are further distinguished into mucus-secreting goblet cells, hormone-secreting enteroendocrine cells (EECs), and, in mammals, antimicrobial-secreting Paneth cells and chemosensing, immunostimulatory tuft cells (Gerbe et al., 2016; Noah and Shroyer, 2013). The mechanisms that drive specific intestinal cell lineages are currently under investigation, but involve signaling between differentiating cells expressing Notch ligands, such as Delta, that activate Notch receptors on adjacent cells; signal-receiving cells become absorptive enterocytes, whereas signal-producing cells become secretory (Koch et al., 2013). In zebrafish, no molecular markers are known for intestinal stem or progenitor cells, but mature secretory cells are distinguished by multiple markers (Fig. 1). Zebrafish are well-suited to the study of vertebrate host-microbe interactions because it is easy to derive large numbers of GF individuals (Melancon et al., 2017), they are optically transparent allowing visualization of both host and microbial cells (Taormina et al., 2012), and they are genetically tractable.

The mechanisms by which microbiota interact with Notch signaling and influence intestinal cell fate are unknown. Studies link Notch signaling to toll-like receptors (TLRs) that detect bacterial components and induce innate immune responses (Palaga et al., 2008; Shang et al., 2016; Zhang et al., 2012) via a conserved adaptor protein, Myd88 (Fre et al., 2011; Stein et al., 2007). We found that Myd88-dependent signaling is required for microbiota to promote zebrafish intestinal epithelial proliferation (Cheesman et al., 2011), suggesting that innate immunity can mediate cell fate responses to intestinal microbes.

Here, we tested the hypothesis that the microbiota promotes secretory fates through Myd88-dependent inhibition of Notch signaling, by examining epistatic relationships between the microbiota, Notch signaling and Myd88-dependent signaling in gnotobiotic zebrafish. We found that modulation of intestinal Notch signaling is downstream of microbial signals that promote secretory fates, and that the microbiota modulates Notch signaling via Myd88. We provide the first evidence that microbiota-induced Myd88-dependent signaling plays a role in Notch-mediated intestinal cell fate determination.

RESULTS AND DISCUSSION

Microbiota-induced Notch signaling promotes intestinal epithelial secretory cell fate determination

We previously showed a paucity of secretory cells in 8 days post-fertilization (dpf) GF zebrafish (Bates et al., 2006). Here, we

[1]Institute of Molecular Biology, Department of Biology, 1229 University of Oregon, Eugene, OR 97403, USA. [2]Institute of Neuroscience, Department of Biology, 1254 University of Oregon, Eugene, OR 97403, USA. [3]Institute of Biology, Leiden University, 2300 RA Leiden, The Netherlands. [4]Children's Cancer Research Institute, 1090 Vienna, Austria. [5]Humans and the Microbiome Program, Canadian Institute for Advanced Research, Toronto, Ontario, Canada M5G 1Z8.
*Present address: Translational Imaging Center, Department of Molecular and Computational Biology, University of Southern California, Los Angeles, CA 90089, USA. ‡Present address: Brain Tumor Immunotherapy Program, Department of Neurosurgery, Duke University, Durham, NC 27710, USA. §Present address: Department of Integrative Biology, Michigan State University, East Lansing, MI 48824, USA. ¶Present address: Institute for Immunology, University of California Irvine, Irvine, CA 92697, USA. **Present address: Department of Pathology, University of Utah, Salt Lake City, UT 84103, USA.

‡‡Authors for correspondence (kguillem@uoregon.edu; eisen@uoneuro.uoregon.edu)

M.K.H., 0000-0003-0293-7043; J.G., 0000-0002-9471-1828; W.Z.S., 0000-0002-8072-9023; E.M., 0000-0002-1050-8217; A.H.M., 0000-0002-1325-0725; M.D., 0000-0001-5942-0817; J.S.E., 0000-0003-1229-1696; K.G., 0000-0001-6004-9955

Received 26 May 2017; Accepted 19 January 2018

Development (2018) 145, dev155317. doi:10.1242/dev.155317

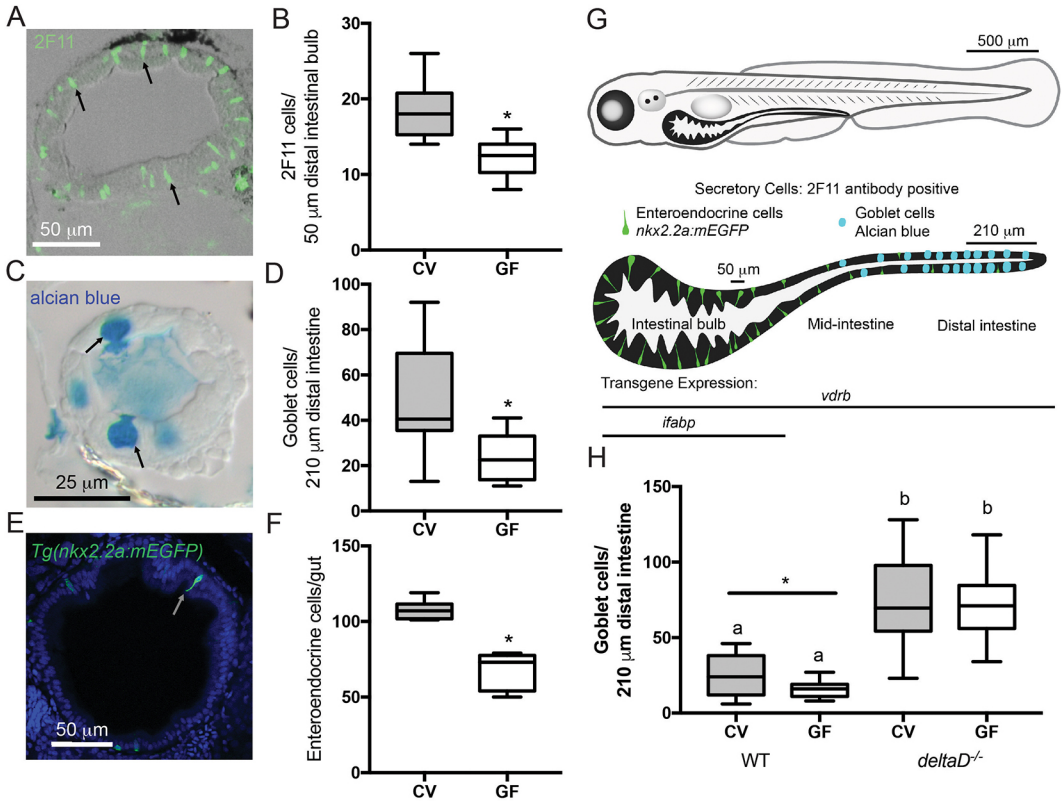

Fig. 1. The microbiota promotes intestinal epithelium secretory cell fates through the Notch ligand DeltaD. (A) Representative image of cross-section stained with 2F11 antibody (e.g. black arrows). (B) Number of 2F11-positive secretory cells in CV and GF larvae; *n*=16. (C) Representative image of mucus-containing vacuole of goblet cells stained with Alcian Blue (black arrows). (D) Counts of Alcian Blue-positive goblet cells in CV and GF larvae; *n*=18 (CV), 14 (GF). (E) Representative cross-section of *Tg(nkx2.2a:mEGFP)* larva expressing GFP in (EECs (white arrow). (F) Number of GFP-positive EECs in GF and CV *Tg(nkx2.2a:mEGFP)* larvae; *n*=6 (CV), 9 (GF). (G) Schematic of larval zebrafish and larvae intestine. Enteroendocrine and goblet secretory cells are indicated in their normal intestinal locations. The transgene *vdrb* is expressed through the entire intestine whereas *ifabp* is expressed only in the bulb. Labeled bars by the isolated intestine schematic indicate the bulb and distal intestine regions scored for 2F11 and Alcian Blue, respectively. (H) Number of Alcian Blue-positive goblet cells in CV and GF WT and *deltaD*$^{-/-}$ larvae; *n*=15 (WT), 12 (CV *deltaD*$^{-/-}$), 13 (GF *deltaD*$^{-/-}$). *P<0.05, Student's *t*-test. Letters denote P<0.05, ANOVA followed by Tukey's post-hoc test. Each box represents the first to third quartiles, center bar the median, and whiskers the maximum and minimum of each dataset.

provide evidence that 7 dpf GF larvae also have fewer secretory cells than their CV siblings, as revealed by 2F11 antibody staining (Fig. 1A,B; Crosnier et al., 2005; Zhang et al., 2014), goblet cell markers (Alcian Blue; Fig. 1C,D) and EEC transgene (*nkx2.2a:mEGFP*) expression (Fig. 1E,F; Pauls et al., 2007). We previously found no difference in the total number of intestinal epithelial cells in GF and CV larvae (Bates et al., 2006), suggesting that the paucity of secretory cells in GF intestines is due to reallocation of cells to the enterocyte fate. Fig. 1G shows a diagrammatic representation of secretory cell types along the length of the intestine (Wallace et al., 2005), and indicates the regions analyzed for Fig. 1A-F and the expression domains of transgenes used in subsequent experiments. Our finding that the GF intestinal epithelium contains fewer secretory cells mirrors reports from GF rats (Tomas et al., 2013; Uribe et al., 1994) and mice (Kandori et al., 1996). Additionally, in fruit flies the microbiota modulates intestinal secretory fate determination through Notch signaling, although in this case Notch signaling is decreased and enteroendocrine cells are more abundant in the GF state (Broderick et al., 2014).

Notch signaling is a key mechanism for cell fate determination throughout the animal kingdom. We combined gnotobiotic and genetic manipulations to test whether the microbiota influences secretory fate via Notch signaling. CV homozygous *deltaD* mutants have many more intestinal epithelial secretory cells than CV wild-type (WT) siblings (Fig. 1H), but not as many as observed in *mind bomb*^{ta52b} zebrafish, which harbor a mutation that abrogates all Notch signaling, causing complete conversion of the intestinal epithelium to the secretory fate (Crosnier et al., 2005). The increased number of goblet cells in CV versus GF WT intestines is consistent with the hypothesis that the microbiota promotes secretory fates by inhibiting Notch signaling; alternatively, there could be a parallel, Notch-independent effect. We reasoned that if microbiota cues that promote goblet cells act in parallel with DeltaD, then we should observe fewer goblet cells in GF than in CV *deltaD* mutants. In contrast, we observed a similarly high number of goblet cells in CV and GF *deltaD* mutant intestines (Fig. 1H), consistent with the model that host perception of microbiota cues requires DeltaD to promote intestinal secretory fate.

Intestinal epithelial Notch signaling is required for microbial-dependent secretory cell fate

To determine whether Notch signaling is necessary in the intestinal epithelium to transduce microbial cues that promote secretory fates, we generated transgenic lines with intestine-specific expression of constructs that constitutively activate or repress Notch signaling. To establish whether intestinal epithelial Notch activation inhibits secretory fates, we used the *Tg(UAS:nicd)* line, which ectopically activates Notch signaling by expressing the Notch intracellular domain under control of the yeast upstream activating sequence (Cambier et al., 2014). To achieve intestine-specific expression, we

Development (2018) 145, dev155317. doi:10.1242/dev.155317

used a transgenic line isolated in a Gal4-enhancer trap screen (Distel et al., 2009) that expresses the yeast Gal4 transcription factor throughout the larval intestinal epithelium (Fig. 2A), including in secretory cells (Fig. S1). We mapped the *GAL4;Tg(UAS:mCherry)* insertion to the vitamin D receptor (*vdrb*) gene, which in mammals is expressed in all intestinal epithelial cells including stem cells (Peregrina et al., 2015). *Tg(vdrb:GAL4)*; *Tg(UAS:ncid)*; *Tg(UAS:mCherry)* larvae had fewer goblet cells compared with sibling *Tg(vdrb:GAL4)*; *Tg(UAS:mCherry)* larvae (Fig. 2B), consistent with our expectation that intestinal epithelial Notch activation is sufficient to inhibit secretory fates and promote absorptive fates.

To confirm an intestine-specific role for Notch signaling in secretory fate specification, we generated a stable line that expresses the *dn-rbpj* transgene, encoding a dominant-negative form of the Notch pathway transcription factor Rbpj, to repress Notch (Guruharsha et al., 2012). We drove intestinal epithelial expression of *dn-rbpj* and a TdTomato reporter, using a 1.8 kb fragment of the intestinal fatty acid binding protein promoter (*ifabp*; *fabp2*) (Her et al., 2004). Using this same *ifabp* promoter element, we previously induced elevated epithelial cell proliferation upon ectopic expression of the *Helicobacter pylori* effector protein CagA (Neal et al., 2013), suggesting that the promoter's expression domain includes intestinal epithelial stem or progenitor cells. Expression of *ifabp:TdTomato:p2a:dn-rbpj* (*ifabp:dn-rbpj*) is restricted to proximal intestinal epithelium (Fig. 2C), where most secretory cells are EECs (Fig. 1G) (Wallace et al., 2005). To assess the effects of Notch signaling modulation on proximal intestinal secretory cell specification, we crossed the EEC marker *Tg(nkx2.2a:mEGFP)* into our transgenic line and quantified GFP-expressing cells in the region expressing TdTomato (Fig. 2D). Consistent with the *ifabp* promoter driving expression of Notch-modulating transgenes in progenitors of mature secretory cells, we observed more EECs in fish expressing *ifabp:dn-rbpj* (Fig. 2E). To exclude the possibility of tissue hyperplasia in *ifabp:dn-rbpj* intestines with elevated EECs, we estimated total epithelial cells by quantifying them in representative transverse sections in three regions [esophageal intestinal junction (eij), intestinal bulb (ib) and mid-intestine (mi)] and observed no differences between *ifabp:dn-rbpj* and WT larvae (Fig. S2).

We next addressed whether microbiota-derived cues promote secretory fates by activating intestinal epithelial Notch signaling. The low number of goblet cells in CV *Tg(vdrb:GAL4)*; *Tg(UAS:ncid)*; *Tg(UAS:mCherry)*-expressing larvae (Fig. 2B), similar to levels in GF WTs (Fig. 1D), is consistent with our model that the microbiota suppresses Notch signaling. However, the low number of goblet cells in both groups made it difficult to assess whether the microbiota affected the *Tg(vdrb:GAL4)*; *Tg(UAS:ncid)*; *Tg(UAS:mCherry)* goblet cell phenotype. In contrast, the high number of EECs in *ifabp:dn-rbpj* larvae (Fig. 2E) provided an informative

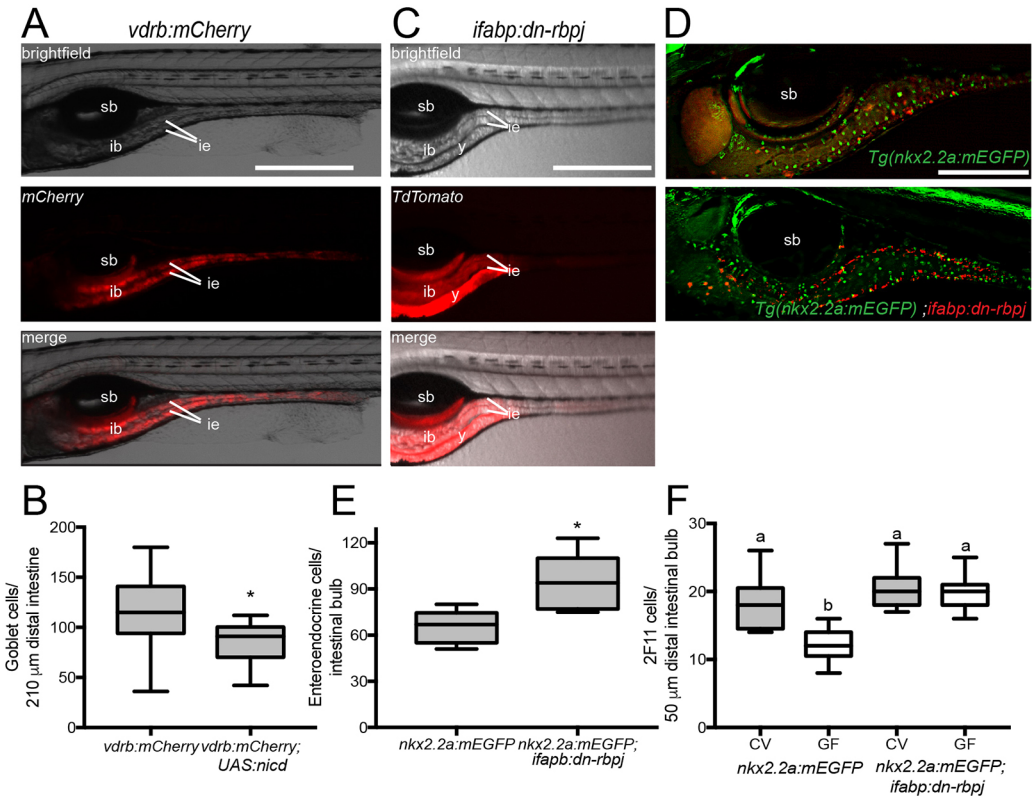

Fig. 2. Modulating Notch signaling within the intestinal epithelium is sufficient to alter secretory cell numbers. (A) Expression of *Tg(vdrb:GAL4)*; *Tg(UAS:mCherry)*; *(vdrb:mCherry)* with brightfield, fluorescence and merged signals; *vdrb:GAL4* is expressed throughout the intestinal epithelium. (B) Number of goblet cells in *vdrb:mCherry* and *vdrb:mCherry*; *Tg(UAS:nicd)* zebrafish. *n*=23 (*vdrb:mCherry*), 10 [*vdrb:mCherry*; *Tg(UAS:nicd)*]. (C) Expression of *ifabp:dn-rbpj* with brightfield, fluorescence and merged signals; note that *ifabp* drives expression primarily in posterior intestinal bulb and proximal intestine. (D) Representative images of *Tg(nkx2.2a:mEGFP)* and *Tg(nkx2.2a:mEGFP)* crossed with *ifabp:dn-rbpj* to determine the effect of modulating Notch on EECs (green) in regions in which Notch signaling is augmented or suppressed (red). (E) Number of EECs in *ifabp:dn-rbpj* larvae; *n*=5 [*Tg(nkx2.2a:mEGFP)*], 7 [*Tg(nkx2.2a:mEGFP)*; *ifabp:dn-rbpj*]. (F) Quantification of 2F11-positive secretory cells in CV and GF *Tg(nkx2.2a:mEGFP)* and *Tg(nkx2.2a:mEGFP)*; *ifabp:dn-rbpj* larvae; *n*=17 for each condition. ib, intestinal bulb; ie, intestinal epithelium; sb, swim bladder; y, yolk. **P*<0.05, Student's *t*-test. Letters denote *P*<0.05, ANOVA followed by Tukey's post-hoc test. Each box represents the first to third quartiles, center bar the median, and whiskers the maximum and minimum of each dataset. Scale bars: 500 μm (A,C); 250 μm (D).

Development (2018) 145, dev155317. doi:10.1242/dev.155317

phenotype for microbiota manipulations. We found that CV and GF *dn-rbpj*-expressing larvae had the same high number of 2F11-positive secretory cells (Fig. 2F), consistent with the microbiota functioning upstream of Rbpj in the Notch pathway within the intestinal epithelium.

The microbiota promotes secretory cell fates by signaling through Myd88

We next addressed how microbiota cues are perceived by the host Notch pathway. We showed previously that the innate immune signaling adaptor Myd88 is responsible for microbiota-dependent developmental processes (Bates et al., 2007; Cheesman et al., 2011). To learn whether Myd88 promotes secretory fates, we used *myd88* mutants with a stop codon at amino acid 85, which results in a prematurely truncated protein containing only the N-terminal death domain (van der Vaart et al., 2013). This *myd88* mutation resulted in fewer goblet cells in both heterozygotes and homozygotes (Fig. 3A), suggesting that it behaves in a dominant-negative manner. Because this mutant was severely immunocompromised and difficult to maintain, we also used a previously validated splice-blocking morpholino (MO) specific to the *myd88* exon2/intron2 boundary (Bates et al., 2007; Cambier et al., 2014). As in *myd88* mutants, MO-mediated reduction of *myd88* expression resulted in fewer goblet cells compared with control siblings (Fig. 3B). One downstream effector of Myd88 is the pro-inflammatory cytokine tumor necrosis factor alpha (TNFα) (Akira and Takeda, 2004). We used previously validated splice-blocking MOs to knock down expression of *tnfrsf1a* (tumor necrosis factor receptor superfamily, member 1a), which encodes the TNF receptor (Bates et al., 2007), and observed fewer goblet cells in MO-injected animals compared with control siblings (Fig. 3C). These data support a requirement for Myd88-dependent signaling to promote intestinal secretory fates.

To test whether Myd88 acts downstream of the microbiota to promote secretory fates, we derived GF *myd88* MO-injected and control mock-injected embryos and compared the secretory cell numbers in larvae reared GF or CVZ after the injections. We observed the expected reduction in secretory cells in GF versus CVZ larvae and found that secretory cell numbers in both CVZ and GF *myd88* MO-injected larvae were comparable to GF controls, and were all significantly lower than the number of secretory cells in control CVZ larvae (Fig. 3D). The absence of an additive reduction in secretory cell number with the combined loss of *myd88* and microbiota suggests that secretory cell-promoting signals from the microbiota are mediated through Myd88.

Myd88 requires intestinal epithelial Notch signaling to promote secretory cell fates

Our epistasis tests of the signaling pathways required for promoting intestinal epithelial secretory fates placed the microbiota upstream of both Myd88 and intestinal epithelial Notch signaling. To determine whether Myd88 acts directly in the Notch pathway, we knocked down Myd88 function in WTs and *deltaD* mutants. We found fewer goblet cells in *myd88* MO-injected WT larvae compared with WT controls. Moreover, we saw an increase in goblet cells in both *myd88* MO-injected and control *deltaD* mutants (Fig. 4A), demonstrating that Myd88 functions upstream of DeltaD to promote goblet cell fates.

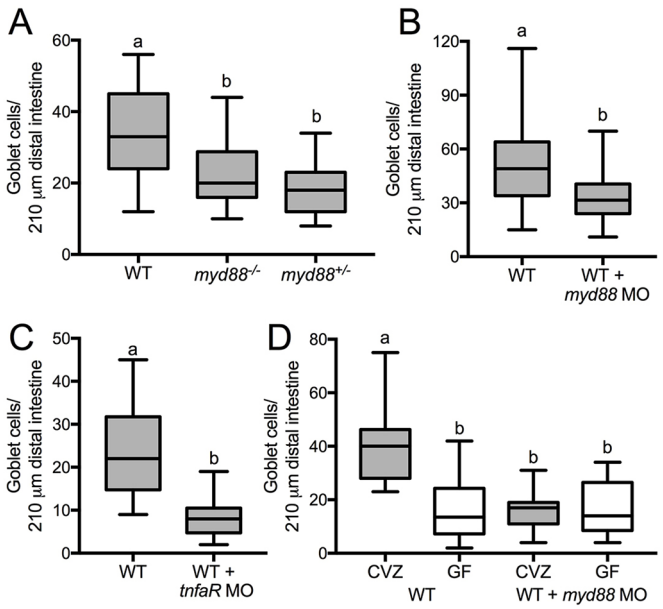

Fig. 3. Myd88-dependent signaling is required for the microbiota to promote goblet cell fate. Alcian Blue-positive goblet cells were counted in multiple conditions. (A) Heterozygous and homozygous *myd88* mutant larvae compared with WT siblings; *n*=17 (WT), 14 (*myd88*$^{-/-}$), 15 (*myd8*$^{+/-}$). (B) *myd88* MO-injected WT larvae; *n*=19 (WT), 22 (WT+*myd88* MO). (C) *tnfrsf1a* MO-injected WT larvae; *n*=14 (WT), 10 (WT+ *tnfaR* MO). (D) WT and *myd88* MO-injected larvae siblings derived CVZ or GF; *n*=14 (CVZ WT), 12 (GF WT), 15 (CVZ WT+*myd88* MO), 13 (GF WT+*myd88* MO). Letters denote *P*<0.05, ANOVA followed by Tukey's post-hoc test. Each box represents the first to third quartiles, center bar the median, and whiskers the maximum and minimum of each dataset.

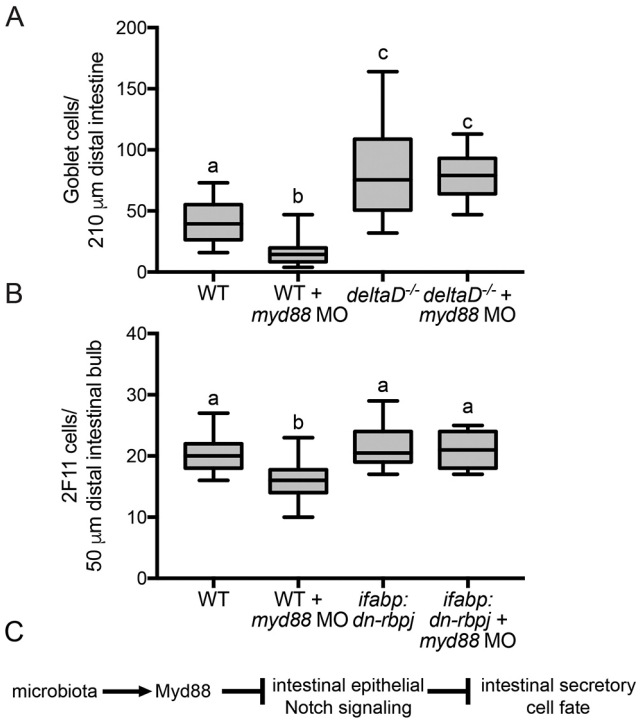

Fig. 4. Myd88 requires Notch signaling to promote goblet cell fates. (A) Number of goblet cells in *myd88* MO-injected WT and *deltaD*$^{-/-}$ larvae; *n*=22 (WT), 20 (WT+*myd88* MO and *deltaD*$^{-/-}$), 19 (*deltaD*$^{-/-}$+*myd88* MO). (B) Number of 2F11-positive secretory cells in *myd88* MO-injected WT and *ifabp:dn-rbpj* larvae; *n*=18. (C) Schematic showing our model that the microbiota interacts with Myd88 to inhibit Notch signaling, which, in turn, inhibits intestinal secretory cell fate. Letters denote *P*<0.05, ANOVA followed by Tukey's post-hoc test. Each box represents the first to third quartiles, center bar the median, and whiskers the maximum and minimum of each dataset.

Development (2018) 145, dev155317. doi:10.1242/dev.155317

Finally, we addressed whether Myd88 requires intestine-specific Notch signaling to promote secretory fates. We compared the effect of Myd88 on secretory cells by injecting *myd88* MO into WT and *ifabp:dn-rbpj* fish. *ifabp:dn-rbpj* larvae with inhibited intestinal epithelial Notch signaling showed no response to MO-mediated *myd88* inhibition (Fig. 4B). Additionally, we confirmed that the change in secretory cell number did not alter total intestinal cells in *myd88* MO-injected fish (Fig. S2).

Microbiota modulation of intestinal epithelial Notch signaling regulates proportions of absorptive and secretory cells

Our results support a model in which the microbiota promotes intestinal secretory fates through Myd88-mediated inhibition of Notch signaling in the intestinal epithelium (Fig. 4C). Myd88 is also required for microbiota activation of Wnt signaling and promoting intestinal epithelial cell proliferation in the zebrafish larval intestine (Cheesman et al., 2011). A subtle distinction between these two phenomena is that Tnfr is required for secretory fate determination and dispensable for normal epithelial cell renewal (Cheesman et al., 2011), but plays a role in pathological, inflammation-associated intestinal epithelial hyperplasia (Rolig et al., 2017). Because Notch and Wnt signaling are intimately coordinated in the balance of intestinal epithelial cell proliferation and differentiation (Sancho et al., 2015), it will be interesting to dissect the microbiota cues that stimulate these different pathways.

Host-microbe interactions involving developmental signaling pathways likely evolved because they provide an advantage to the host and its resident microbiota. In the vertebrate intestine, secretory cells are crucial for shaping the environment to foster controlled microbial growth and confer protection against microbial insults. Goblet cells secrete mucus that creates a barrier between luminal contents and epithelial cells, and also provides microbiota with habitats and nutrients (Desai et al., 2016; Johansson and Hansson, 2016; Kashyap et al., 2013). EECs impact the intestinal environment through secretion of over 30 peptide hormones (Vincent et al., 2011) that aid digestion and absorption (Tolhurst et al., 2012), glucose metabolism (Pais et al., 2016), and motility (Sikander et al., 2009). Motility in turn can profoundly impact the microbiota (Rolig et al., 2017; Wiles et al., 2016).

Secretory cells shape the resident microbes' intestinal environment and emerging evidence suggests they also are sensors for microbial products. For example, goblet cells respond to both host factors, such as acetylcholine, and microbial factors, through host innate signaling receptors, including NLRP6 (Birchenough et al., 2015; Wlodarska et al., 2014) and Myd88 (Knoop et al., 2017, 2015; Miller et al., 2014). Similarly, EECs are luminal sensors of microbiota (Bogunovic et al., 2007) and short chain fatty acids (Gribble and Reimann, 2016; Reigstad et al., 2015), which may prime the host immune system during intestinal dysbiosis (Worthington, 2015). The Myd88-dependent sensing of microbiota cues we describe here might be mediated by secretory cells, which could modulate Notch signaling in the tissue to maintain an appropriate census of secretory cells for the organ's microbial environment. Our results suggest that development of at least two secretory cell types, goblet cells and EECs, are subject to similar genetic and environmental controls. It would be interesting to learn whether there are additional regional and cell type-specific processes involved that affect development of these cells in distinct ways along the length of the gut.

Not only is Notch signaling required for cell fate determination in the developing intestine, but it also plays crucial roles in tissue homeostasis throughout life (Sancho et al., 2015). For example, mice with intestinal epithelial-specific deletion of Rbpj exhibit impaired barrier function and develop microbiota-dependent spontaneous colitis (Obata et al., 2012). On the other end of the spectrum, mice overexpressing intestinal epithelial claudin 1 exhibit increased Notch signaling, loss of goblet cells and protective mucus, and increased sensitivity to dextran sulfate sodium-induced colitis (Pope et al., 2014). The finding that resident microbiota can modulate host intestinal epithelial Notch signaling offers the potential for new therapeutic approaches to target this crucial pathway to promote intestinal health throughout life.

MATERIALS AND METHODS

Animal husbandry, gnotobiology and genetics

Experiments were conducted according to protocols approved by the University of Oregon Institutional Animal Care and Use Committee and followed standard zebrafish protocols (Westerfield, 2007). GF embryos were generated by surface sterilization (Bates et al., 2007, 2006), and then reared without feeding in sterile embryo media in tissue culture flasks. Experiments were conducted at 7 dpf, rather than at 8 dpf as in Bates et al. (2006), to reduce possible nutrient deprivation secondary effects. Sterility was verified by plating the media to count colony forming units (CFUs) and by visual inspection through a compound microscope. CV fish were naturally spawned sibling embryos not subjected to surface sterilization and instead kept in UO Zebrafish Facility system water but were otherwise reared under the same conditions as GF counterparts. We verified that media chemistry (pH, conductivity, ammonia, nitrates, nitrites, alkalinity) was the same for GF, CV and CVZ conditions.

Generation of the *ifabp:TdTomato:p2a:dn-rbpj* (*ifabp:dn-rbpj*) transgenic line was accomplished using splicing by overlap extension (SOE) PCR as described further in the supplementary Materials and Methods. Briefly, a construct in which a 1.8 kb region of the *ifabp* promoter sequence (Table S1) drove the expression of *TdTomato* and *dn-rbpj* was generated using primers presented in Table S2.

myd88 and *tnfrsf1a* MO-injected animals were generated as described previously (Bates et al., 2007) and detailed further in the supplementary Materials and Methods. Briefly, splice-blocking MOs (Gene Tools) were injected into embryos at the one-cell stage. Morpholino sequences are presented in Table S3 and splice blocking was verified by RT-PCR using the primers in Table S4. For GF derivation of *myd88* MO-injected animals, embryos were generated by *in vitro* fertilization in antibiotic-containing embryo media (Pham et al., 2008). Embryos were injected at the one-cell stage, derived GF, and then a portion of the population immediately conventionalized by immersion in UO Zebrafish Facility system water containing zebrafish-associated bacteria (Stephens et al., 2016). AB/Tü was the WT reference for all experiments.

deltaD^{tr233} mutants were maintained as homozygotes (Holley et al., 2000; Jiang et al., 1996) and out-crossed with WT every other generation. Homozygous *deltaD*^{tr233} mutant embryos were identified by somite defects (Holley et al., 2000). *myd88*^{hu3568} mutants were maintained as homozygotes and identified by a PCR reaction showing a single base pair mutation at bp 390 from a T to an A (van der Vaart et al., 2013). The *vdrb:GAL4;UAS:mCherry* line was isolated in a Gal4-enhancer trap screen (Distel et al., 2009) and was maintained as a homozygous line. The *vdrb:GAL4* insertion site was identified using a method similar to that developed to identify bacterial transposon insertion sites (Langridge et al., 2009), as described in the supplementary Materials and Methods using primers presented in Table S5.

Histological analysis

Details of histological analysis are provided in the supplementary Materials and Methods. Briefly, to quantify goblet cells, 7 dpf larvae were fixed in 4% paraformaldehyde in PBS overnight at 4°C, stained with 0.04% Alcian Blue (Sigma-Aldrich), embedded in paraffin, cut in 7 µm transverse sections and mounted on glass slides. We estimated total epithelial cells by staining sections with DAPI and counting nuclei in three different regions [esophageal intestinal junction (eij), intestinal bulb (ib), and mid-intestine (mi)].

Statistics

All secretory cell counting experiments were performed a minimum of two times with at least n=10. Absolute numbers of secretory cells varied between experiments, possibly owing in part to fluctuations in the composition of the CV microbiota; however, the trends in relative abundance of secretory cells between treatment groups were consistent across experiments. When only two groups were compared, significance was determined using Student's t-test assuming unequal variances. When more than two groups were compared, significance was determined using ANOVA and Tukey's pairwise comparisons, family error rate=0.05. All statistics were performed using the JMP9 software package.

Acknowledgements

Thanks to Erika Mittge, Rose Sockol, and the UO Zebrafish Facility staff for technical support.

Competing interests

The authors declare no competing or financial interests.

Author contributions

Conceptualization: J.V.T., J.M.B., J.S.E., K.G.; Methodology: J.V.T., M.L.A., J.G., J.M.B., W.Z.S., E.M.; Validation: J.V.T.; Formal analysis: J.V.T., M.K.H.; Investigation: J.V.T.; Resources: M.V., A.H.M., M.D., J.S.E., K.G.; Data curation: J.S.E., K.G.; Writing - original draft: J.V.T., M.K.H.; Writing - review & editing: J.V.T., M.K.H., J.G., W.Z.S., E.M., J.S.E., K.G.; Visualization: J.V.T., M.K.H.; Supervision: J.S.E., K.G.; Project administration: J.V.T., M.K.H.; Funding acquisition: J.V.T., J.S.E., K.G.

Funding

Research reported in this publication was supported by an American Cancer Society postdoctoral fellowship (120188-PF-11-272-01-MPC to J.V.T.), and the National Institutes of Health (32DK089716 to J.V.T.; P01HD22486 and P50GM098911 to J.S.E. and K.G.). Deposited in PMC for release after 12 months.

Supplementary information

Supplementary information available online at
http://dev.biologists.org/lookup/doi/10.1242/dev.155317.supplemental

References

Akira, S. and Takeda, K. (2004). Toll-like receptor signalling. *Nat. Rev. Immunol.* **4**, 499-511.

Bates, J. M., Mittge, E., Kuhlman, J., Baden, K. N., Cheesman, S. E. and Guillemin, K. (2006). Distinct signals from the microbiota promote different aspects of zebrafish gut differentiation. *Dev. Biol.* **297**, 374-386.

Bates, J. M., Akerlund, J., Mittge, E. and Guillemin, K. (2007). Intestinal alkaline phosphatase detoxifies lipopolysaccharide and prevents inflammation in zebrafish in response to the gut microbiota. *Cell Host Microbe* **2**, 371-382.

Birchenough, G. M. H., Johansson, M. E. V., Gustafsson, J. K., Bergström, J. H. and Hansson, G. C. (2015). New developments in goblet cell mucus secretion and function. *Mucosal. Immunol.* **8**, 712-719.

Bogunovic, M., Davé, S. H., Tilstra, J. S., Chang, D. T. W., Harpaz, N., Xiong, H., Mayer, L. F. and Plevy, S. E. (2007). Enteroendocrine cells express functional Toll-like receptors. *Am. J. Physiol. Gastrointest. Liver Physiol.* **292**, G1770-G1783.

Broderick, N. A., Buchon, N. and Lemaitre, B. (2014). Microbiota-induced changes in drosophila melanogaster host gene expression and gut morphology. *MBio* **5**, e01117-14.

Cambier, C. J., Takaki, K. K., Larson, R. P., Hernandez, R. E., Tobin, D. M., Urdahl, K. B., Cosma, C. L. and Ramakrishnan, L. (2014). Mycobacteria manipulate macrophage recruitment through coordinated use of membrane lipids. *Nature* **505**, 218-222.

Cheesman, S. E., Neal, J. T., Mittge, E., Seredick, B. and Guillemin, K. (2011). Epithelial cell proliferation in the developing zebrafish intestine is regulated by the Wnt pathway and microbial signaling via Myd88. *Proc. Natl. Acad. Sci. USA* **108 Suppl 1**, 4570-4577.

Crosnier, C., Vargesson, N., Gschmeissner, S., Ariza-McNaughton, L., Morrison, A. and Lewis, J. (2005). Delta-Notch signalling controls commitment to a secretory fate in the zebrafish intestine. *Development* **132**, 1093-1104.

Desai, M. S., Seekatz, A. M., Koropatkin, N. M., Kamada, N., Hickey, C. A., Wolter, M., Pudlo, N. A., Kitamoto, S., Terrapon, N., Muller, A. et al. (2016). A dietary fiber-deprived Gut microbiota degrades the colonic mucus barrier and enhances pathogen susceptibility. *Cell* **167**, 1339-1353.e21.

Distel, M., Wullimann, M. F. and Koster, R. W. (2009). Optimized Gal4 genetics for permanent gene expression mapping in zebrafish. *Proc. Natl. Acad. Sci. USA* **106**, 13365-13370.

Fre, S., Bardin, A., Robine, S. and Louvard, D. (2011). Notch signaling in intestinal homeostasis across species: the cases of Drosophila, Zebrafish and the mouse. *Exp. Cell Res.* **317**, 2740-2747.

Gerbe, F., Sidot, E., Smyth, D. J., Ohmoto, M., Matsumoto, I., Dardalhon, V., Cesses, P., Garnier, L., Pouzolles, M., Brulin, B. et al. (2016). Intestinal epithelial tuft cells initiate type 2 mucosal immunity to helminth parasites. *Nature* **529**, 226-230.

Gribble, F. M. and Reimann, F. (2016). Enteroendocrine cells: chemosensors in the intestinal epithelium. *Annu. Rev. Physiol.* **78**, 277-299.

Guruharsha, K. G., Kankel, M. W. and Artavanis-Tsakonas, S. (2012). The Notch signalling system: recent insights into the complexity of a conserved pathway. *Nat. Rev. Genet.* **13**, 654-666.

Her, G. M., Yeh, Y.-H. and Wu, J.-L. (2004). Functional conserved elements mediate intestinal-type fatty acid binding protein (I-FABP) expression in the gut epithelia of zebrafish larvae. *Dev. Dyn.* **230**, 734-742.

Holley, S. A., Geisler, R. and Nusslein-Volhard, C. (2000). Control of her1 expression during zebrafish somitogenesis by a delta-dependent oscillator and an independent wave-front activity. *Genes Dev.* **14**, 1678-1690.

Jiang, Y. J., Brand, M., Heisenberg, C. P., Beuchle, D., Furutani-Seiki, M., Kelsh, R. N., Warga, R. M., Granato, M., Haffter, P., Hammerschmidt, M. et al. (1996). Mutations affecting neurogenesis and brain morphology in the zebrafish, Danio rerio. *Development* **123**, 205-216.

Johansson, M. E. V. and Hansson, G. C. (2016). Immunological aspects of intestinal mucus and mucins. *Nat. Rev. Immunol.* **16**, 639-649.

Kandori, H., Hirayama, K., Takeda, M. and Doi, K. (1996). Histochemical, lectin-histochemical and morphometrical characteristics of intestinal goblet cells of germfree and conventional mice. *Exp. Anim.* **45**, 155-160.

Kashyap, P. C., Marcobal, A., Ursell, L. K., Smits, S. A., Sonnenburg, E. D., Costello, E. K., Higginbottom, S. K., Domino, S. E., Holmes, S. P., Relman, D. A. et al. (2013). Genetically dictated change in host mucus carbohydrate landscape exerts a diet-dependent effect on the gut microbiota. *Proc. Natl. Acad. Sci. USA* **110**, 17059-17064.

Knoop, K. A., McDonald, K. G., McCrate, S., McDole, J. R. and Newberry, R. D. (2015). Microbial sensing by goblet cells controls immune surveillance of luminal antigens in the colon. *Mucosal Immunol.* **8**, 198-210.

Knoop, K. A., Gustafsson, J. K., McDonald, K. G., Kulkarni, D. H., Kassel, R. and Newberry, R. D. (2017). Antibiotics promote the sampling of luminal antigens and bacteria via colonic goblet cell associated antigen passages. *Gut Microbes* **8**, 1-12.

Koch, U., Lehal, R. and Radtke, F. (2013). Stem cells living with a Notch. *Development* **140**, 689-704.

Langridge, G. C., Phan, M.-D., Turner, D. J., Perkins, T. T., Parts, L., Haase, J., Charles, I., Maskell, D. J., Peters, S. E., Dougan, G. et al. (2009). Simultaneous assay of every Salmonella Typhi gene using one million transposon mutants. *Genome Res.* **19**, 2308-2316.

McFall-Ngai, M., Hadfield, M. G., Bosch, T. C. G., Carey, H. V., Domazet-Lošo, T., Douglas, A. E., Dubilier, N., Eberl, G., Fukami, T., Gilbert, S. F. et al. (2013). Animals in a bacterial world, a new imperative for the life sciences. *Proc. Natl. Acad. Sci. USA* **110**, 3229-3236.

Melancon, E., Gomez De La Torre Canny, S., Sichel, S., Kelly, M., Wiles, T. J., Rawls, J. F., Eisen, J. S. and Guillemin, K. (2017). Best practices for germ-free derivation and gnotobiotic zebrafish husbandry. *Methods Cell Biol.* **138**, 61-100.

Miller, M. J., Knoop, K. A. and Newberry, R. D. (2014). Mind the GAPs: insights into intestinal epithelial barrier maintenance and luminal antigen delivery. *Mucosal Immunol.* **7**, 452-454.

Neal, J. T., Peterson, T. S., Kent, M. L. and Guillemin, K. (2013). H. pylori virulence factor CagA increases intestinal cell proliferation by Wnt pathway activation in a transgenic zebrafish model. *Dis. Model. Mech.* **6**, 802-810.

Noah, T. K. and Shroyer, N. F. (2013). Notch in the intestine: regulation of homeostasis and pathogenesis. *Annu. Rev. Physiol.* **75**, 263-288.

Obata, Y., Takahashi, D., Ebisawa, M., Kakiguchi, K., Yonemura, S., Jinnohara, T., Kanaya, T., Fujimura, Y., Ohmae, M., Hase, K. et al. (2012). Epithelial cell-intrinsic Notch signaling plays an essential role in the maintenance of gut immune homeostasis. *J. Immunol.* **188**, 2427-2436.

Pais, R., Gribble, F. M. and Reimann, F. (2016). Stimulation of incretin secreting cells. *Ther. Adv. Endocrinol. Metab.* **7**, 24-42.

Palaga, T., Buranaruk, C., Rengpipat, S., Fauq, A. H., Golde, T. E., Kaufmann, S. H. E. and Osborne, B. A. (2008). Notch signaling is activated by TLR stimulation and regulates macrophage functions. *Eur. J. Immunol.* **38**, 174-183.

Pauls, S., Zecchin, E., Tiso, N., Bortolussi, M. and Argenton, F. (2007). Function and regulation of zebrafish nkx2.2a during development of pancreatic islet and ducts. *Dev. Biol.* **304**, 875-890.

Peregrina, K., Houston, M., Daroqui, C., Dhima, E., Sellers, R. S. and Augenlicht, L. H. (2015). Vitamin D is a determinant of mouse intestinal Lgr5 stem cell functions. *Carcinogenesis* **36**, 25-31.

Pham, L. N., Kanther, M., Semova, I. and Rawls, J. F. (2008). Methods for generating and colonizing gnotobiotic zebrafish. *Nat. Protoc.* **3**, 1862-1875.

Pope, J. L., Bhat, A. A., Sharma, A., Ahmad, R., Krishnan, M., Washington, M. K., Beauchamp, R. D., Singh, A. B. and Dhawan, P. (2014). Claudin-1

regulates intestinal epithelial homeostasis through the modulation of Notch-signalling. *Gut* **63**, 622-634.
Reigstad, C. S., Salmonson, C. E., Rainey, J. F., III, Szurszewski, J. H., Linden, D. R., Sonnenburg, J. L., Farrugia, G. and Kashyap, P. C. (2015). Gut microbes promote colonic serotonin production through an effect of short-chain fatty acids on enterochromaffin cells. *FASEB J.* **29**, 1395-1403.
Rolig, A. S., Mittge, E. K., Ganz, J., Troll, J. V., Melancon, E., Wiles, T. J., Alligood, K., Stephens, W. Z., Eisen, J. S. and Guillemin, K. (2017). The enteric nervous system promotes intestinal health by constraining microbiota composition. *PLoS Biol.* **15**, e2000689.
Sancho, R., Cremona, C. A. and Behrens, A. (2015). Stem cell and progenitor fate in the mammalian intestine: Notch and lateral inhibition in homeostasis and disease. *EMBO Rep.* **16**, 571-581.
Shang, Y., Smith, S. and Hu, X. (2016). Role of Notch signaling in regulating innate immunity and inflammation in health and disease. *Protein Cell* **7**, 159-174.
Sikander, A., Rana, S. V. and Prasad, K. K. (2009). Role of serotonin in gastrointestinal motility and irritable bowel syndrome. *Clin. Chim. Acta* **403**, 47-55.
Stein, C., Caccamo, M., Laird, G. and Leptin, M. (2007). Conservation and divergence of gene families encoding components of innate immune response systems in zebrafish. *Genome Biol.* **8**, R251.
Stephens, W. Z., Burns, A. R., Stagaman, K., Wong, S., Rawls, J. F., Guillemin, K. and Bohannan, B. J. M. (2016). The composition of the zebrafish intestinal microbial community varies across development. *ISME J.* **10**, 644-654.
Taormina, M. J., Jemielita, M., Stephens, W. Z., Burns, A. R., Troll, J. V., Parthasarathy, R. and Guillemin, K. (2012). Investigating bacterial-animal symbioses with light sheet microscopy. *Biol. Bull.* **223**, 7-20.
Tolhurst, G., Reimann, F. and Gribble, F. M. (2012). Intestinal sensing of nutrients. *Handb. Exp. Pharmacol.***209**, 309-335.
Tomas, J., Wrzosek, L., Bouznad, N., Bouet, S., Mayeur, C., Noordine, M.-L., Honvo-Houeto, E., Langella, P., Thomas, M. and Cherbuy, C. (2013). Primocolonization is associated with colonic epithelial maturation during conventionalization. *FASEB J.* **27**, 645-655.
Uribe, A., Alam, M., Johansson, O., Midtvedt, T. and Theodorsson, E. (1994). Microflora modulates endocrine cells in the gastrointestinal mucosa of the rat. *Gastroenterology* **107**, 1259-1269.
van der Vaart, M., van Soest, J. J., Spaink, H. P. and Meijer, A. H. (2013). Functional analysis of a zebrafish myd88 mutant identifies key transcriptional components of the innate immune system. *Dis. Model. Mech.* **6**, 841-854.
Vincent, K. M., Sharp, J. W. and Raybould, H. E. (2011). Intestinal glucose-induced calcium-calmodulin kinase signaling in the gut-brain axis in awake rats. *Neurogastroenterol. Motil.* **23**, e282-e293.
Wallace, K. N., Akhter, S., Smith, E. M., Lorent, K. and Pack, M. (2005). Intestinal growth and differentiation in zebrafish. *Mech. Dev.* **122**, 157-173.
Westerfield, M. (2007). *The Zebrafish Book. A Guide for the Laboratory Use of Zebrafish (Danio rerio)*, 5th edn. Eugene: Univ. of Oregon Press.
Wiles, T. J., Jemielita, M., Baker, R. P., Schlomann, B. H., Logan, S. L., Ganz, J., Melancon, E., Eisen, J. S., Guillemin, K. and Parthasarathy, R. (2016). Host gut motility promotes competitive exclusion within a model intestinal microbiota. *PLoS Biol.* **14**, e1002517.
Wlodarska, M., Thaiss, C. A., Nowarski, R., Henao-Mejia, J., Zhang, J.-P., Brown, E. M., Frankel, G., Levy, M., Katz, M. N., Philbrick, W. M. et al. (2014). NLRP6 inflammasome orchestrates the colonic host-microbial interface by regulating goblet cell mucus secretion. *Cell* **156**, 1045-1059.
Worthington, J. J. (2015). The intestinal immunoendocrine axis: novel cross-talk between enteroendocrine cells and the immune system during infection and inflammatory disease. *Biochem. Soc. Trans.* **43**, 727-733.
Yuan, X., Wu, H., Xu, H., Xiong, H., Chu, Q., Yu, S., Wu, G. S. and Wu, K. (2015). Notch signaling: an emerging therapeutic target for cancer treatment. *Cancer Lett.* **369**, 20-27.
Zhang, Q., Wang, C., Liu, Z., Liu, X., Han, C., Cao, X. and Li, N. (2012). Notch signal suppresses Toll-like receptor-triggered inflammatory responses in macrophages by inhibiting extracellular signal-regulated kinase 1/2-mediated nuclear factor kappaB activation. *J. Biol. Chem.* **287**, 6208-6217.
Zhang, D., Golubkov, V. S., Han, W., Correa, R. G., Zhou, Y., Lee, S., Strongin, A. Y. and Dong, P. D. S. (2014). Identification of Annexin A4 as a hepatopancreas factor involved in liver cell survival. *Dev. Biol.* **395**, 96-110.

Supplemental Experimental Procedures

Transgenic line generation

ifabp:tdtomato:p2a:dn-rbpj (*ifabp:dn-rbpj*): the *dn-rbpj* sequence was amplified from *pDONR221-su[H]dn1*. Using *pDestTol2pA2* as the backbone, a *tol2* destination vector was generated by using an *ifabp* 5' entry vector (Table S1), with a pME entry vector to introduce *tdTomato* and a *p2A:notch* 3' entry vector. The *p2A:notch* fusions were accomplished using SOE PCR using primers *attB2/5'p2a*, *3'p2A/5'suHdn_R*, *5' suHdn_F*, and *attB3/3' suHdn_R* (Table S2) resulted in a sequence containing *attB2:P2A-dnRBPj:attB3*. The PCR fragment was then recombined into the gateway Donor vector *pDONR P2r-P3* following manufacturer's instructions (Invitrogen, Carlsbad, CA). The 3' entry plasmid was used in multi-site gateway reactions with the *p5E:ifabp* and *pMEtdTomato* plasmids and recombined into *pDestTol2pA2* according to manufacturer's instructions (Invitrogen, Carlsbad, CA); the resulting construct carried *ifabp:tdtomato:p2a:dn-rbpj*.

The *ifabp:dn-rbpj* construct was microinjected into AB/Tu embryos at the 1-cell stage for tol2-mediated transgenesis as previously described (Kwan et al., 2007) and allowed to develop normally. Larvae were screened for GFP expression in the heart and tdTomato expression in the intestinal epithelium at 7-8 dpf. Individuals expressing both markers were reared to adulthood and kept as stable transgenic lines.

Morpholino injections

myd88 and *tnfR* MO-injected animals were generated as previously described (Bates et al., 2007). Splice blocking morpholinos (Gene Tools, Philomath, OR) were

injected into embryos at the one cell stage. The *myd88*e212 morpholino was injected at 5 pmol per embryo. To knockdown *tnfR,* the *TR1v1/TR1v2* morpholinos were injected at 1.2 pmol and 6 pmol respectively (Bates et al., 2007). Mock-injected controls where injected with only phenol red and water. Morpholino sequences are presented in Table S3. Splice-blocking was verified by RT-PCR using the primers in Table S4. For both morpholinos, efficacy of target knock down was also assessed by assaying for reduction of intestinal myeloid peroxidase activity positive neutrophils to GF levels, as described (Bates et al., 2007).

Histological analysis

To determine goblet cell numbers, fixed larvae were washed 3x 10 min in Phosphate Buffered Saline (PBS) and equilibrated in 100 mM Tris pH7.5, 10 mM $MgCl_2$ for 10 min. Goblet cells were labeled with 0.04% Alcian Blue (Sigma Aldrich, St. Louis, MO), 10 mM $MgCl_2$ in Ethanol for 4 d at room temperature. Labeled larvae were then rehydrated and destained with successive 5 min washes of 100 mM Tris pH7.5, 10 mM $MgCl_2$ in 80%, 50% and 25% Ethanol. Paraffin-embedded larvae were sectioned in 7 μm thick slices and goblet cells were counted in 30 sections retrograde from the vent.

2F11 antibody (ab71286; 1:500; ABCAM, Cambridge, MA) staining in histological sections was performed as previously described (Crosnier et al., 2005). The 2F11 antibody recognizes the pan-secretory cell antigen Annexin 4A (Zhang et al., 2014). 7 dpf larvae were fixed in 1% formaldehyde for 3 h at room temperature. Larvae were then washed 3x for 10 min with PBS, blocked in Saponin Block Buffer: PBS, 1% BSA (Sigma Aldrich, St. Louis, MO), 1% DMSO (Sigma Aldrich, St. Louis, MO), 0.5%

Saponin (Sigma Aldrich, St. Louis, MO), 2% Goat Serum (Jackson Immunoresearch, West Grove, PA). Larvae were then incubated with the 2F11 antibody diluted 1:1000 in Saponin Block Buffer at 4°C overnight, followed by 4 1h washes with PBS + 1% Triton-X-100. AlexaFluor488-conjugated goat anti-Rabbit secondary antibodies (Life Technologies, Grand Island, NY) were diluted into Saponin Block buffer and incubated with the larvae overnight at 4°C followed by 3x 30 min washes with PBS + 1% Triton-X-100 and 3x 5 min washes in PBS. 2F11 stained secretory cells in whole mount larvae were visualized on a Leica (DFC360FX) fluorescence stereo microscope. All 2F11 stained secretory cells within a 50 μm length of the intestinal bulb were counted.

EECs were directly enumerated on a Leica fluorescence stereo dissection scope (Leica DFC360FX). 7 dpf *nkx2.2a:egfp;ifabp:dn-rbp-j* larvae were anaesthetized and mounted in 4% methyl cellulose on glass slides. All GFP positive cells within the region of intestinal tdTomato expression were counted and compared against WT sibling controls.

Identification of the vdrb:GAL4 *genomic insertion site*

The *vdrb:GAL4* insertion site was identified using a method similar to that developed to identify transposon insertion sites in bacteria (Stephens et al., 2015). Briefly, 1.5 μg of genomic DNA was pooled from 14 individual larvae and sheared to a median fragment size of 300 bp, end-repaired with NEB Quick-blunting kit (New England Biolabs, Ipswich, MA), then cleaned up and A-tailed using Klenow Fragment (3'->5' exo-) (New England Biolabs, Ipswich, MA). Standard paired-end Illumina adapters with T-overhangs were then ligated to the DNA fragments with T4 ligase (New

England Biolabs, Ipswich, MA) overnight at room temperature. The ligation reaction was then cleaned up with a Qiagen (Germantown, MD) MinElute column to remove excess adapter sequences. 28 ng of the cleaned ligation was used as template in a 50 ul PCR using Phusion high-fidelity polymerase (cycling conditions: 1:00 initial denature at 98 C followed by 30 cycles of 98 C for 10 seconds, 56 C for 30 seconds, 72 C for 20 seconds, followed by final extension at 72 C for 2 minutes). The forward primer (*tol2_addP5*; Table S5) was designed to add a 5 nucleotide barcode and full-length Illumina adapter sequence while targeting a 22 bp sequence of the tol2 construct (CCCTAAGTACTTGTACTTTCAC) located 34 bp from the transposon end. The reverse primer (*P7_amp*; Table S5) targeted the asymmetric ends of the ligated Illumina adapters that would not contain a priming site for the reverse primer unless the forward primer had extended its template. The PCR product was run on a 1.5% agarose gel and a fragment in the range of 150-300 bp was extracted. The final Illumina library was spiked in as a small portion of another Illumina library and run on a single lane of the Illumina GAII. Raw sequences were first identified by their 5 nucleotide barcode and the presence of the primer sequence used to target the tol2 construct, then end-trimmed and quality filtered to remove low quality base calls at the end of sequences as well as low-quality sequences overall. The remaining 34 bp of the tol2 construct end sequence that was not directly targeted by the primer was used to identify reads that came from amplified products that correctly targeted the tol2 construct integrated into the genome. As expected, the accuracy of the targeting primer (forward) was low, with only 3.2% of the quality reads that contained the target primer sequence also containing the 34 bp of the untargeted tol2 construct end sequence. Finally, after filtering out Illumina adapter

sequences, the potential genomic insertion site was identified in each read as the sequence after the tol2 inverted repeat (TIR) sequence at the transposon end. These 1608 potential genomic insertion site sequences were aligned to the Zv9 build of the zebrafish genome with Bowtie2 (Langmead and Salzberg, 2012). Of the 1596 quality alignments, all but 1 aligned to the same zebrafish genomic sequence (Zv9 build chromosome 6:38936157) located in the first intron of the *vdrb* gene (ENSEMBL Gene ID ENSDARG00000070721) suggesting there was only a single tol2 insertion in this transgenic line. To independently verify the insertion site, we designed primers that anneal to the *vdrb* gene and the tol2 construct (vdrbGal4_check and tol2_out, Table S5) so that we would amplify a 794 bp fragment only if the identified insertion site was correct. All of the original 14 individuals were tested and showed the expected amplification. Sanger sequencing of the amplified products confirmed the predicted insertion site, identifying the tol2 construct ends adjacent to the predicted zebrafish genomic sequence (*vdrb:GAL4* insertion site sequence).

References

Bates, J.M., Akerlund, J., Mittge, E., and Guillemin, K. (2007). Intestinal alkaline phosphatase detoxifies lipopolysaccharide and prevents inflammation in zebrafish in response to the gut microbiota. Cell Host Microbe *2*, 371-382.

Crosnier, C., Vargesson, N., Gschmeissner, S., Ariza-McNaughton, L., Morrison, A., and Lewis, J. (2005). Delta-Notch signalling controls commitment to a secretory fate in the zebrafish intestine. Development *132*, 1093-1104.

Kwan, K.M., Fujimoto, E., Grabher, C., Mangum, B.D., Hardy, M.E., Campbell, D.S., Parant, J.M., Yost, H.J., Kanki, J.P., and Chien, C.B. (2007). The Tol2kit: a multisite gateway-based construction kit for Tol2 transposon transgenesis constructs. Dev Dyn *236*, 3088-3099.

Langmead, B., and Salzberg, S.L. (2012). Fast gapped-read alignment with Bowtie 2. Nat Methods *9*, 357-359.

Stephens, W.Z., Wiles, T.J., Martinez, E.S., Jemielita, M., Burns, A.R., Parthasarathy, R., Bohannan, B.J., and Guillemin, K. (2015). Identification of Population Bottlenecks and Colonization Factors during Assembly of Bacterial Communities within the Zebrafish Intestine. MBio *6*, e01163-01115.

Zhang, D., Golubkov, V.S., Han, W., Correa, R.G., Zhou, Y., Lee, S., Strongin, A.Y., and Dong, P.D. (2014). Identification of Annexin A4 as a hepatopancreas factor involved in liver cell survival. Dev Biol *395*, 96-110.

Table S1. *ifabp:dn-rbpj* promoter sequence

atcactgttacgcagattctgcaaattctacaaaatgtttgtagtaaatatagtataaaagatgtttttagcttacttttttacattattt
tatacatttaaacatgcatgaaatcaattattatcagcttggacctttttcttgtccctactcttagtgggacgatgccaaaggtctt
acaatgggacgataccaaaggtcttcagaggtcttatttaattgcactgttaagagattaaggataaggtaatgatgagataa
accatcatcagagattatcatgtctcagtttgatatctcgtctctttatcttgtcatggagcctccagataaaacttccacactgc
atgttgcttaatttgaatcatttgcaggctttgtacactattcatcattacagataatgctgaagctgttctttcacagccttgcatc
aatatttacaacattttcaaacaatacaaggggataattcagtaatacaatttaaaataaggttccaataactatattactaataa
ctaacaatgagcaaaatacataatgctgttatttttagtataactggatgagtactgcagattttaaataaaatattcatggaatta
ttgtcgttactgtataatgttggtgaatgtatggtctgtttttgacatttgtgtgcatttatttttatatctaaagtgttttatagatttgca
ttttaatattagtagtaaatgcaaatgataaatactttatctttaaattaaaaatattattatgcattacttatctgtgataaatatatc
gtatgtgttatgttactgataaaatgttacaataataatggttcggttagggttaaggttttaggacaaaacacaactgttcatta
gtattcagatcagatctatgaaataatattggcaggtgcaaattttcattttaataatgtactagtactgtaaatatttgagttagct
ttagaactggctttgaagtatattcactggtagctgtctgttaagtagaactgcacaaaaaaaaggtacgaggaagaacgaa
gcattgccatatactgtattctcaattttagctgcaatagctgcacttttgtagtaaaaagttcttcaaagacccttttttatatagtg
tgaagaacttttcaataatcttaaaacatttttctacataaataaaatttttgtgcaatgaaatatttcaaaaagtactttataaaac
caaccattcatgtcaacacagagccttaaaataattgttaccagtatttctcaatagccaatgaggcatgcagcaagattgta
aactaatttaactgtaaccattaaatctaaagttttgacctttgacctttcaccacaattgtttaaaaatcaatacatgtggctaga
attcatagctttcaaacactcttcatagtccctcagtagttactgcaacacaaggcacttactagtataacagacacaccctac
acagtttaaacagcaaacaattcaaacaaaagcaggactttgttatgagaacaacagagcgtgtatgtttgaccatcgcagt
acaagtgagtgcttgttctcaggacttgaaatctccgctctttgcacaatcaatgaataagcaaggcatgctgggatgtgtgt
aacatatagcctgttgggcgggtgagatttatacttggtgagctttactcggccacatcagcatgaagataatactcagataa
ggcaacgcttcgccactcgcacaggtataaaagagtggctcggggtaaagttaggccactgtcaggatcacacaacag

Table S2. Primer sequences used for *ifabp* line

Name	Sequence
attB2/5'p2a	GGG GAC AGC TTT CTT GTA CAA AGT GG
3'p2A/5'suHdn_R	GGA ATG CCA GGT TGT GCC ATA GGA C
5' suHdn_F	ATG GCA CAA CCT GGC ATT CC
attB3/3' suHdn_R	GGG GAC AAC TTT GTA TAA TAA AGT TG

Table S3. Morpholino sequences

Name	Sequence
*myD88*e2i2	5′-GTTAAACACTGACCCTGTGGATCAT-3′
TRlv1	5′-TACGTCCTTGTGCATTGCTGGCATC-3′
TRlv2	5′-CTGCATTGTGACTTACTTATCGCAC-3′

Table S4. Splice-blocking primers

Name	Sequence
MyD88elF	5′-TCTTGACGGACTGGGAAACTCG-3′
MyD88e5R	5′-GATTTGTAGACGACAGGGATTAGCC-3′
TR1F	5′-GCATGGATCCATATCAGGACTTGGTGGA-3′
TR1R	5′-TCGAGAATTCTTACGAAACGCTTGTGTT-3′

Table S5. Primer sequences used for tol2 insertion site identification

Name	Sequence
tol2_addP5	AATGATACGGCGACCACCGAGATCTACACTCTTTCCCTA CACGACGCTCTTCCGATCTXXXXX**CCCTAAGTACTTGTA CTTTCA*C**
P7_amp	CAAGCAGAAGACGGCATACGA
vdrbGal4_check	TAAACACCGACCTTGGCGAG
tol2_out	ACTTTGAGTAGCGTGTACTGGC

XXXXX: 5 nucleotide barcode
*: Phosphorothioate bond
BOLD: Sequence targeting inside tol2 transposon

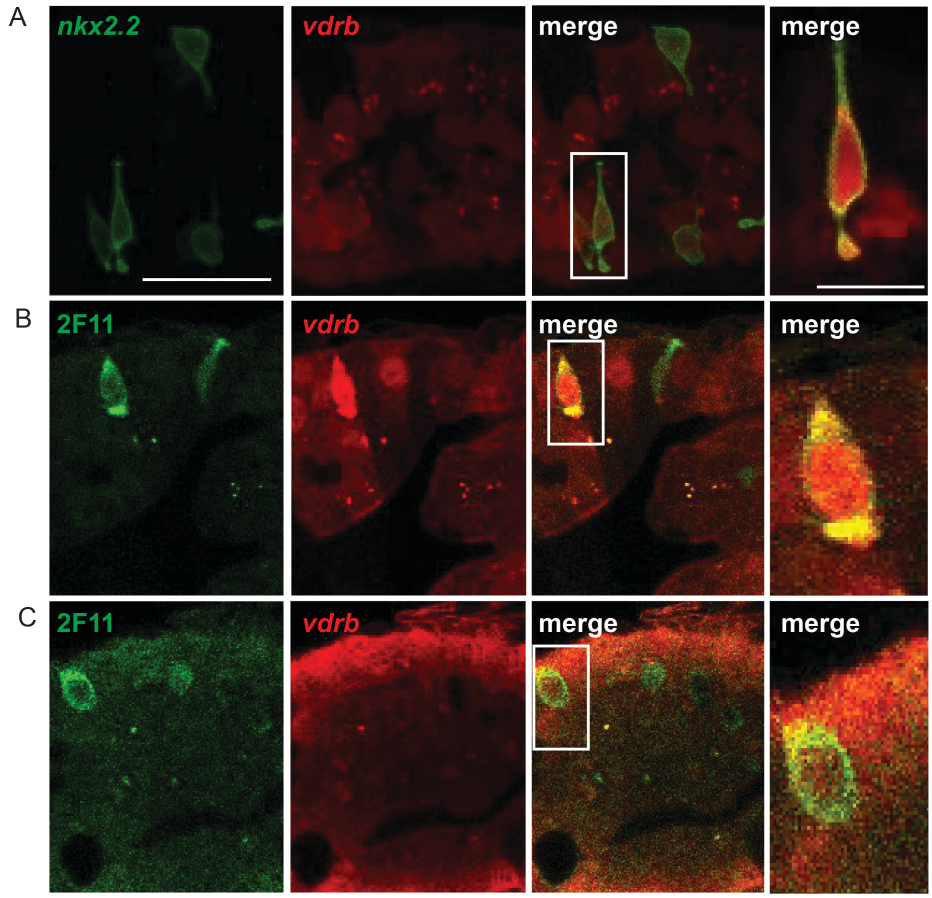

Figure S1. *Tg*(*vdrb:GAL4); Tg(UAS:mCherry*) expression throughout the larval intestinal epithelium, including in secretory cells. Co-expression of the enteroendocrine specific *Tg*(*nkx2.2a:mEGFP)* transgene with *UAS:mCherry* driven by the *vdrb:GAL4* transgene [*Tg(vdrb:mCherry)*] (A). *Tg*(*vdrb:mCherry*) stained with secretory cell marker 2F11 showing expression in both enteroendocrine cells (B) and goblet cells (C). Each image is a single confocal plane. Scale bar = 25 μm in all panels except the three on the far right. Scale bar for the three panels on the far right = 10μm.

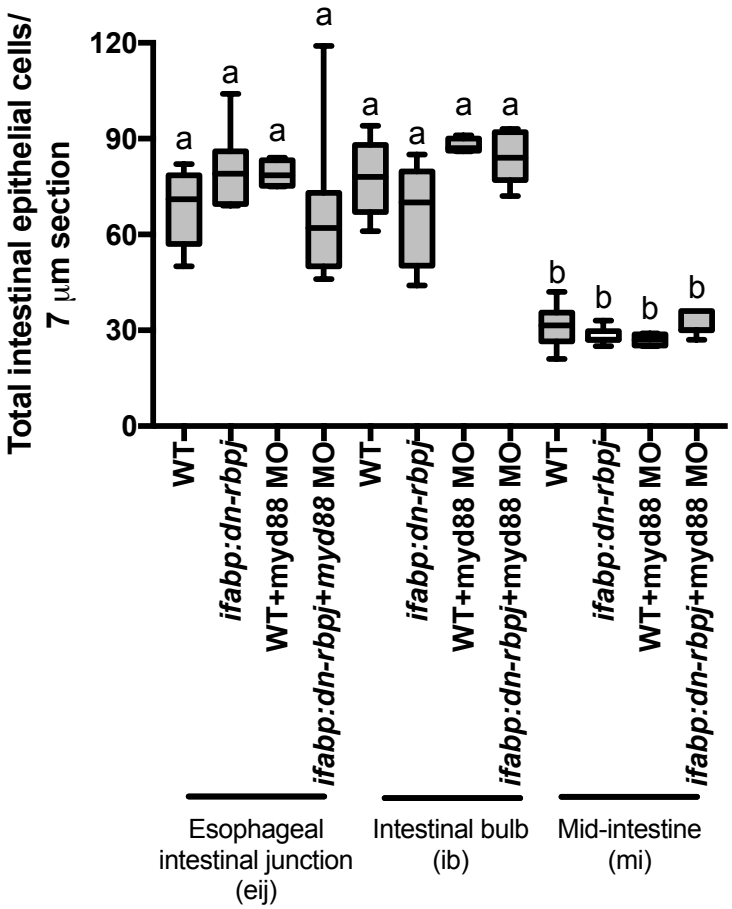

Figure S2. The number of total epithelial cells differs due to larval intestinal region, but not fish or treatment type.